INTERNATIONAL JOURNAL OF INTEGRATED ENGINEERING
ISSN: 2229-838X e-ISSN: 2600-7916

IJIE

Vol. 17 No. 6 (2025) 84-96
https://publisher.uthm.edu.my/ojs/index.php/ijie

Development of 2.4 GHz/3.5 GHz Bowtie Slot Antenna for 5G Communication System

Richard Ting Sing Wee[1], Intan Sorfina Zainal Abidin[1]*, Azniza Abd Aziz[2]

[1] *School of Electrical and Electronic Engineering, Universiti Sains Malaysia, Nibong Tebal, 14300, Penang, MALAYSIA*

[2] *Intel Microelectronics, 11900 Penang, MALAYSIA*

*Corresponding Author: intan.sorfina@usm.my
DOI: https://doi.org/10.30880/ijie.2025.17.06.007

Article Info

Received: 26 March 2025
Accepted: 28 October 2025
Available online: 30 December 2025

Keywords

Bowtie slot antenna, defected ground structure, 5G

Abstract

Driven by the rapid growth and advancements in 5G communication, this research presents the the design, development, and optimization of of dual-band bowtie slot antenna integrated with asymmetrical coplanar waveguide (ACPW) and defected ground structure (DGS). Several combinations and different shape of DGS, such as rectangular and circular slots were studied and compared in this research work. Operating at the crucial Wi-Fi frequency (2.4 GHz) and 5G frequency (3.5 GHz), the antenna's performance, particularly the reflection coefficient, was significantly improved by the inclusion of the DGS. A parametric study confirmed the DGS's positive impact on the simulated impedance matching, reflection coefficient (reaching almost -70 dB in all design with DGS) and bandwidth. The best resuts were given by the bowtie slot antenna integrated with rectangular and circular slots, the reflection coefficient is -70.1 dB (2.4 GHz) and -59.5 dB (3.5 GHz). The -10 dB bandwidths are 602 MHz (2.4 GHz) with fractional bandwidth around 25% and 848 MHz (3.5 GHz) with fractional bandwidth around 24.2%. It was found that the excellent reflection coefficient performance is due to the disruption of surface current distribution caused by the defected structure on the ground plane. The surface current was forced to flow surrounding the DGS, causing it to peak along the DGS edges. Placement of the DGS is also important as it was found that positioning it under the feedline helps to minimize the antenna's mutual coupling.

1. Introduction

The emergence of 5G technology has spurred a growing demand for innovative antenna designs capable of supporting the diverse requirements of this advanced communication system. One critical aspect of 5G is the need to accommodate the exponential increase in data traffic and the proliferation of connected devices [1,2]. To address these challenges, researchers have explored the potential of operating in higher frequency bands, such as the 3.5 GHz range, which is being utilized in several countries for 5G deployment [3]. Moreover, the 2.4 GHz band remains an important frequency for 5G applications, particularly in the context of wireless communication within vehicle environments [4]. Recent advancements in microwave antenna technology have yielded promising solutions for the next generation 5G/6G devices, including the development of reconfigurable antenna systems, phased arrays, and innovative materials such as graphene.

Prior research suggests the 3.4 to 3.8 GHz band is likely the primary frequency for vehicular wireless communication [5]. Multi-band technologies like WiMAX (2.5 GHz/3.5 GHz/5.8 GHz) and WLAN (2.4 GHz/5 GHz)

This is an open access article under the CC BY-NC-SA 4.0 license.

are also rising in popularity nowadays. The unlicensed 2.4 GHz WLAN frequency band is common in homes, while the 3.5 GHz WiMAX band has wide global recognition [6]. A previous study in [6] developed a dual-band (2.4 GHz/3.5 GHz) microstrip antenna integrating a circular patch and U-slot. At present, dual-band antennas are gaining popularity due to their ability to transmit and receive on two frequencies [7]. This research, therefore, focuses on the dual-band operation of the bowtie slot antenna at two commonly used frequencies, the 2.4 GHz and 3.5 GHz.

Bowtie-shaped antennas were proposed previously in other studies mainly for their multiband advantage. For example, the bowtie-shaped microstrip antenna in [8] was used to detect breast cancer. Furthermore, the bowtie antenna was proposed by other researchers in [9] to be used as an ultrawideband antenna. In [10], the bowtie-shaped microstrip antenna was implemented with DGS in order to suppress the unwanted band.

It is widely known that slot antenna has several benefits, and it is mainly associated as a bandwidth enhancement technique. Slot antennas in particular have garnered a lot of attention because of their small size, simplicity in construction, and superior performance, particularly in the millimeter-wave and microwave frequency bands [11]. They can be integrated into metallic objects, enabling discreet communication with a compact transmitter [12,13]. Furthermore, microstrip antennas integrated with printed slots in them are in trend currently due to their low complexity structure, cost-effective, reduced power consumption, easy to fabricate, and can enable significantly high data rates transmission [14,15]. Nevertheless, traditional slot antenna only modestly enhances the patch antenna's narrow bandwidth, typically operate on a single band and exhibits low gain issues. Consequently, in this research work, defected ground structure (DGS) method was incorporated, enabling dual band operation and significantly reducing the antenna's reflection coefficient.

Geometrically compact slots called defective ground structures (DGS) are incorporated into the ground plane of microwave components like antennas and filters. These structures are made up of either several periodic arrangements or a single unit cell [16]. The integration of defected ground structures has been shown to enhance the performance of microstrip antennas, improving characteristics such as bandwidth, impedance matching, and radiation patterns. Integrating DGS is thought to enhance the effective line impedance hence achieving the necessary impedance matching in microwave circuits [17]. For example, a bat-shaped DGS has been utilized to enhance antenna impedance matching [18]. Additionally, to further enhance the antenna's performance, multiple DGS structures were utilized compared to using a single DGS [19]. In [20], the proposed bowtie slot antenna with DGS has better bandwidth enhancement by up to 4.3 times compared to the antenna design without DGS.

Recognizing these needs, this research focuses on the design and development of the dual-band bowtie slot antenna integrated with multiple defected ground structure (DGS) to support 5G communication systems. Their performance was investigated and compared. The suggested antenna in this work operates at 2.4 GHz as well as 3.5 GHz, as these frequency bands are commonly utilized for Wi-Fi and 5G communication systems.

It is worth to note that the research work mentioned in [21] was previously published in a conference proceeding by the same authors as the work presented in this paper. The work in [21] is now used as the preliminary work and is extended to this research paper to study and investigate the effects of inserting defected structure onto the ground plane intended for antenna performance enhancement. Further explanation and antenna evolution are discussed in the subsequent sections.

2. Development of Bowtie Slot Antenna with Dual Band Operation

The simulated top view of the bowtie slot antenna design is displayed in Figure 1 which was previously presented in the research in [21]. Initially, a bowtie-shaped slot was inserted onto the microstrip patch antenna to produce a dual band operation. However, the design exhibits higher reflection coefficient and lower bandwidth with unbalanced port impedance, creating a single band operation. Therefore, the design was improved by adding an asymmetrical coplanar waveguide (ACPW) structure to one of the feedlines as shown in Fig. 1 [22]. The ACPW is designed to provide longer feeding to one of the bowtie slots and is being compacted using a meander technique. The W1 length controls the physical and electrical length of the ACPW while length A controls the placement of the ACPW. The gap SW is optimized to provide the necessary impedance matching for the antenna at 2.4 GHz. This is proven in Fig. 5 whereby the ACPW structure successfully improved the reflection coefficient and impedance matching performance at both frequency bands, 2.4 GHz and 3.5 GHz, producing antenna operating at dual frequency bands. In Fig. 1, the substrate is FR-4 (green), with dielectric constant, ε_r = 4.3 and 1.6 mm thickness while the conductor is copper (yellow), with a thickness, h = 0.035mm.

In this paper, several DGS shape and combination were investigated. Their effect on the performance of the designed bowtie slot antenna will be studied. The evolution of several proposed antenna designs with different DGS is shown in Fig. 2. The study began with Design A by introducing a horizontal rectangular-shaped DGS that seems to cut off the ground plane into two different sections. It was selected as the shape was the easiest and simplest shape as a preliminary work. In Design B which was presented in [21], another slightly smaller vertical rectangular slot was inserted to further enhance the bowtie slot antenna's reflection coefficient's performance. Finally, the smaller rectangular slot was replaced with a circular slot in Design C. The difference in performance of both smaller rectangular and circular slots will be compared later in the next section. The dimensions of all antenna designs proposed in this work are presented in Table 1. The total size of all antennas is maintained at 64.1 x 37.5 mm. In this research work, the ground structure is much bigger than the antenna patch. This is because larger ground plane dramatically enhances the antenna's S_{11} and directivity performance, providing stronger coupling from the patch antenna to the ground plane.

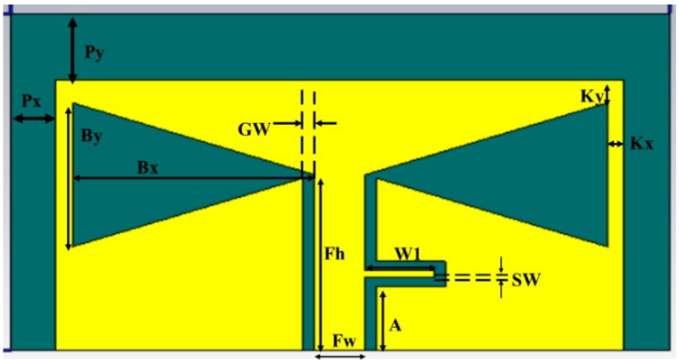

Fig. 1 *Top view of the dual band bowtie slot antenna [21]*

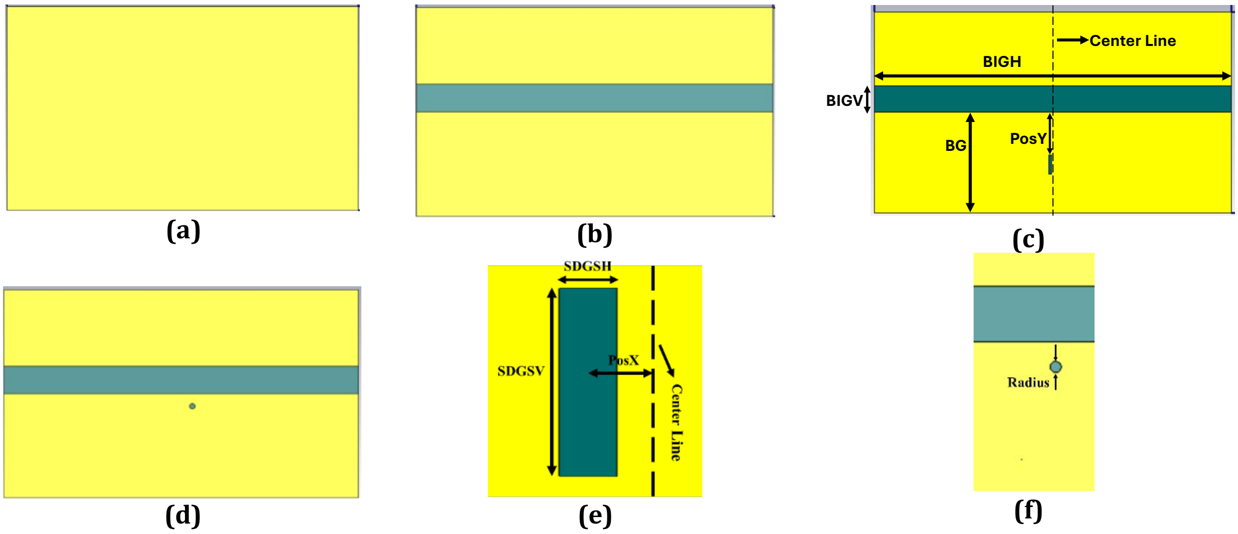

Fig. 2 *Evolution of antenna design with DGS, the bottom view of (a) full ground without DGS; (b) Design A; (c) Design B [21]; (d) Design C; (e) closed up view of Design B vertical slot with dimensions [21]; (f) closed up view of Design C circular slot with dimensions*

Table 1 *Dimensions of bowtie slot antenna with full ground and in design A, B and C*

Parameters	Dimension (mm)	Parameters	Dimension (mm)
Gw	1	BIGV	5
Fh	19.5	BG	18.75
Fw	2	PosX	0.5
Bx	25.05	SW	1.4
By	16	Kx	1.5
Px	4.5	Ky	2.5
Py	7.5	BIGH	64.1
A	7.2	PosY	8
W1	3.4	SDGSV	3.5
Circle radius	0.5	SDGSH	0.5

3. Simulated Results of Bowtie Slot Antenna with Dual Band Operation

3.1 Parametric Study

A study on the important parameters involved in the dual band bowtie slot antenna design is discussed in this section. In all the antenna designs proposed in this work, the bowtie slot antenna design on the top surface is consistent and maintained the same. The most important parameter at the top surface that affects the bowtie antenna's impedance matching is the position of ACPW. The length of A, which is the distance of the ACPW from the bottom edge of the antenna, was varied from 6.2 to 8.2 mm, as shown in Fig. 3. It is observed in Fig. 3 that it has the optimum reflection coefficient for both operating bands with S11 approximately -69 dB at 2.4 GHz and -68 dB at 3.5 GHz when A is 7.2 mm [21]. This is because, the ACPW successfully produced an additional slot path, that increased the cascaded total capacitance of the circuit and have an effect on the resonant frequency of the antenna [22].

Next, the parameters of the DGS on the bottom surface were investigated to determine which parameter affects the antenna's performance the most. From Fig. 4, it can be seen that parameters like BIGH, BIGV, BG and SDGSH affected the antenna performance greatly while parameters like SDGSV, circle radius, posX and posY only affected the reflection coefficient and did not shift the resonant frequency.

Fig. 4(a), (b) and (c) display the parameter of the larger horizontal DGS in Design A. In Fig. 4(a), the resonant frequency, S_{11} and -10 dB bandwidth of the antenna were shifted when the length of BIGH was varied [21]. Only when the BIGH length is at the maximum length at 64.1 mm, the -10 dB bandwidth of the antenna is no longer narrow, a dual band operation is produced, and the S11 is reduced. This proves that the length of the horizontal DGS is important and successfully disrupts the flow of current on the antenna's ground, creating a greater impedance matching response. In Figure 4(b), the length of BIGV, which is the width of the horizontal rectangular DGS, shows that the antenna has the best reflection coefficient and operating at targeted frequency when it is set at 5 mm. The position of the horizontal rectangular slot was also investigated in Fig. 4(c). The position of the slot, which refers to the length of BG, is set at 18.75 mm as the performance shows that it has the best reflection coefficient and resonated at the intended dual band frequencies. It can be observed that the operating frequency of the antenna shifted to higher frequency at 2.8 and 3.7 GHz as the length of BG increased.

Fig. 4(d), (e), (g) and (h) display the parametric study of the smaller vertical rectangular slot in Design B. In Fig. 4(d), when the length of SDGSH, which is the width of the vertical rectangular slot, is 0.5 mm, the operating frequency is located exactly at 2.4 GHz and 3.5 GHz and the antenna has the most optimum reflection coefficient. The resonant frequency of the antenna is shifted to higher frequencies as the length of SDGSH is increased, while the reflection coefficient is worsened. Fig. 4(e) displays the parametric study of SDGSV, the length of the smaller rectangular slot. Adding another rectangular slot successfully lowers the reflection coefficient even further to around -65 dB at lower operating band and -66 dB at higher operating frequency. The position of the smaller rectangular slot was also studied. As can be observed in Fig. 4(g) and (h), varying PosX and PosY helps to improve the reflection coefficient performance while maintaining both operating frequencies. The finalized values of PosX and PosY are 4 mm and 8 mm as they gave the lowest S_{11} and closest to the intended operating frequencies.

In Design C, the radius of the circular slot was added to the horizontal rectangular slot, replacing the vertical horizontal slot. The intention was to study and compare the difference in performance between rectangle shaped-DGS and circle shaped-DGS. The performance of the antenna is the optimum when the circle radius is set 0.5 mm. By replacing with a circular slot, the reflection coefficient is able to reach -70 dB, surpassing the performance of Design B.

In conclusion, dimensions of DGS such as A, BIGH, BIGV, SDGSH and BG have significant effect on the performance of the reflection coefficient of the bowtie slot antenna. Thus, it is important to find the suitable parameter for the antenna to be operated in targeted operating frequency.

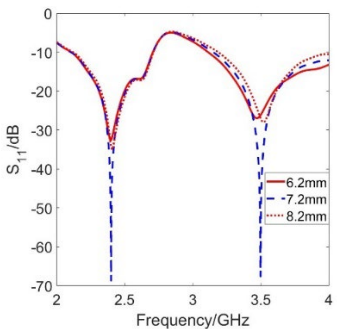

Fig. 3 *Parametric study when varying different lengths of A (the position of ACPW) [21]*

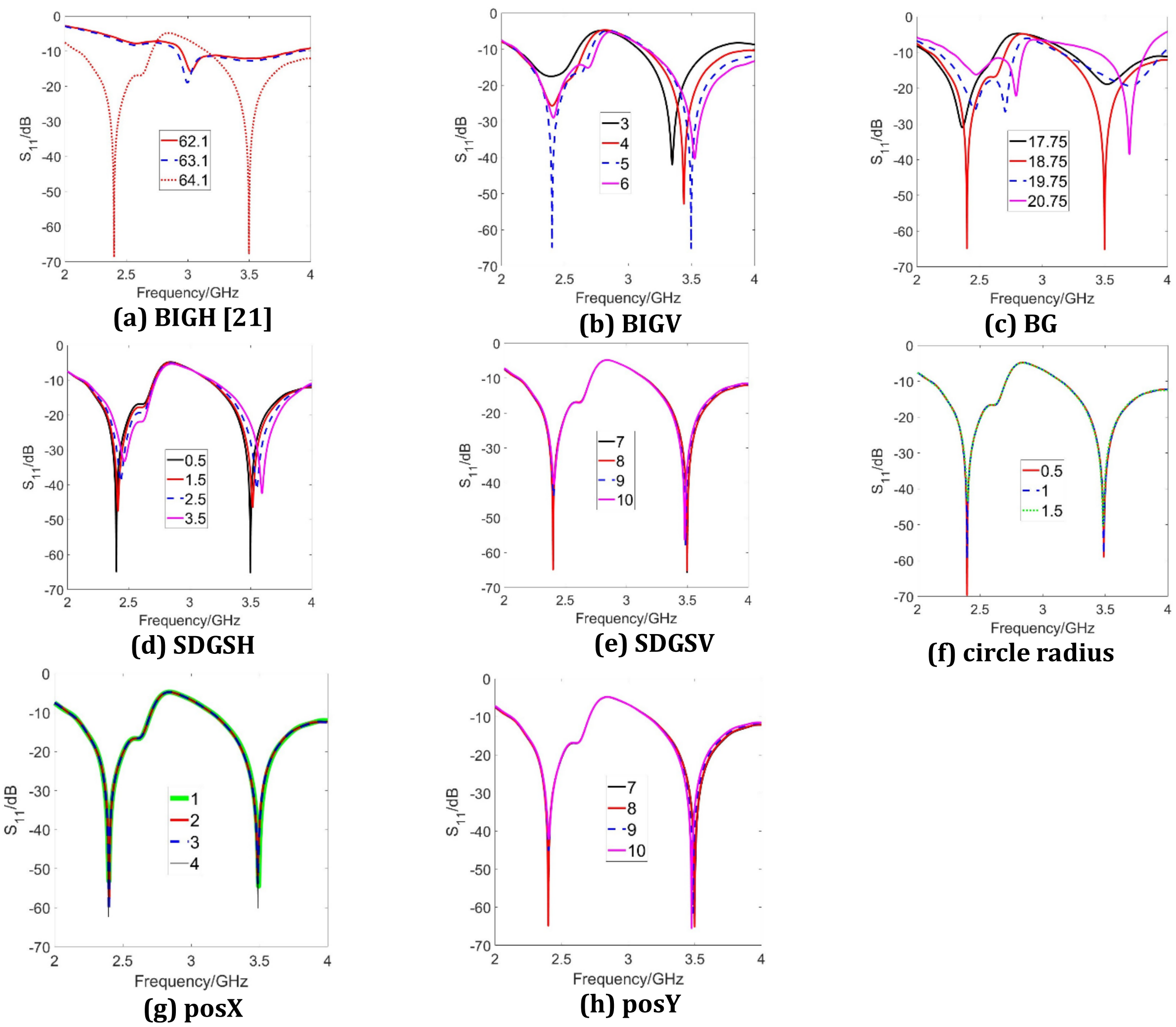

Fig. 4 *Parametric study when varying DGS parameters on the bottom surface*

3.2 Final Results and Discussion

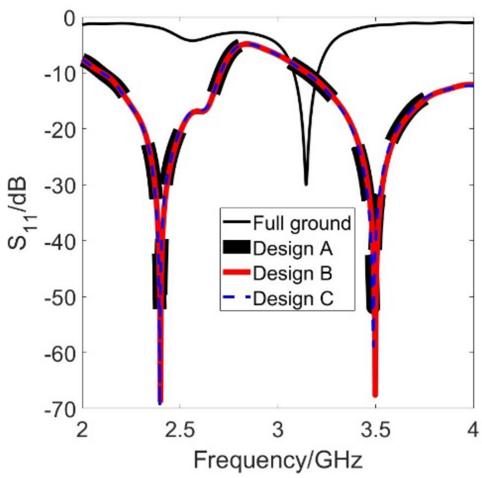

Fig. 5 *Simulated S_{11} of the bowtie slot antenna for full ground (no DGS), Design A (single Big DGS), Design B (big rectangular DGS and small rectangular DGS) and Design C (rectangular+circle)*

Fig. 5 shows the comparison of the optimized simulated S_{11} performance of the bowtie slot antenna with full ground (as the reference design), Design A, Design B and Design C. From Fig. 5, it is observed that Design A, Design

B and Design C are able to operate at 2.4 GHz and 3.5 GHz, creating a dual frequency operating antenna. The reference design, which is the full ground antenna, however, is not able to achieve the dual band operation and only resonated at around 3.2 GHz.

Design A was able to optimize the simulated reflection coefficient's performance with 2.4 GHz frequency band having a reflection coefficient of -40.2 dB and 3.5 GHz frequency band having a reflection coefficient of -52.5 dB. The -10 dB bandwidths are 596.5 MHz at 2.4 GHz with fractional bandwidth around 24.9% and 849.9 MHz at 3.5 GHz with fractional bandwidth around 24.3%. Compared to the reference antenna with full ground, Design A successfully created a dual band operation with much lower S_{11}. The DGS introduced in the proposed bowtie antenna successfully disrupted the current flow on the bottom surface of the antenna and increased the cascaded capacitance of the design, hence bringing the impedance matching closer to 50 Ω.

For Design B, the antenna has a simulated S_{11} of -68.7 dB and -67.9 dB at 2.4 GHz and 3.5 GHz respectively [21]. The -10 dB bandwidths are about 604 MHz at 2.4 GHz with fractional bandwidth around 25.1% and around 845 MHz at 3.5GHz with fractional bandwidth around 24.1%. This shows that by adding another rectangular slot, the reflection coefficient is further lowered, and the bandwidth is slightly enhanced.

In Design C, the reflection coefficient is around -70.1 dB at 2.4 GHz while at 3.5 GHz, the reflection coefficient is around -59.5 dB. The -10 dB bandwidths are 602 MHz at 2.4 GHz with fractional bandwidth around 25% and 848 MHz at 3.5 GHz with fractional bandwidth around 24.2%. This shows that by introducing a circular slot, only the reflection coefficient performance is enhanced but the bandwidth performance remains the same.

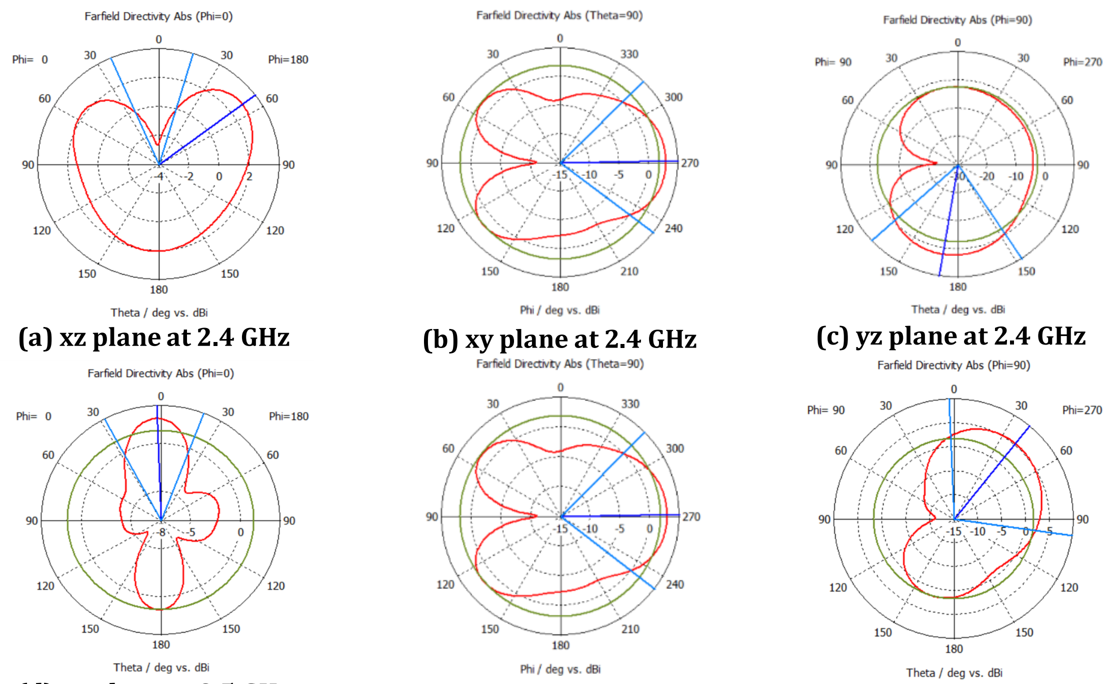

(a) xz plane at 2.4 GHz (b) xy plane at 2.4 GHz (c) yz plane at 2.4 GHz

(d) xz plane at 3.5 GHz (e) xy plane at 3.5 GHz (d) yz plane at 3.5 GHz

Fig. 6 *Simulated 2D radiation pattern of reference bowtie slot antenna with full ground plane*

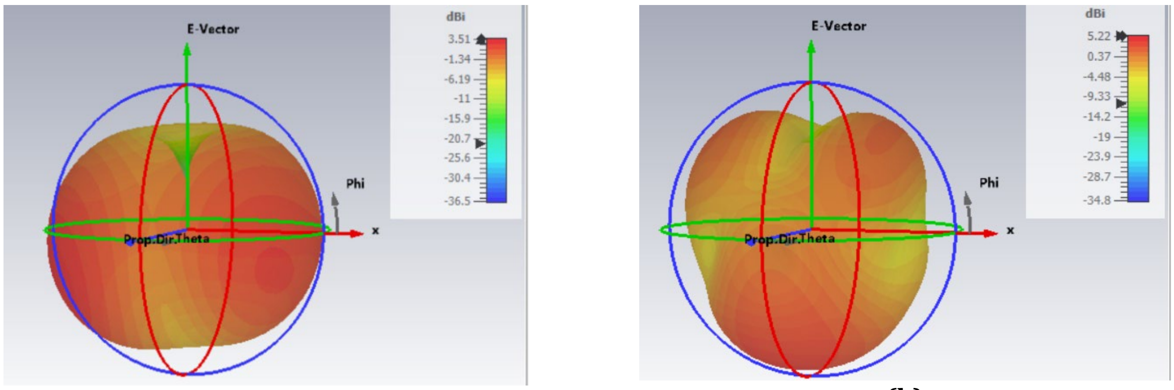

(a) (b)

Fig. 7 *Simulated 3D radiation pattern of reference bowtie slot antenna full ground at (a) 2.4 GHz; (b) 3.5 GHz*

Fig. 6 and 7 present the simulated 2-dimensional (2D) and 3-dimensional (3D) radiation pattern results for the reference bowtie slot antenna with full ground at 2.4 GHz and 3.5 GHz. The antenna has a directivity of 2.16 dBi at 2.4 GHz and its 3 dB beamwidth is 310 degrees. This shows that the full ground antenna is behaving almost like an omnidirectional antenna with a very wide half-power beamwidth at 2.4 GHz. The antenna has a directivity of around 5.22 dBi at 3.5 GHz, and its 3 dB beamwidth is around 45 degrees. At this frequency, the antenna is behaving like a highly directional antenna.

Fig. 8 and 9 display the simulated 2D and 3D radiation pattern results for the antenna with Design A at 2.4 GHz and 3.5 GHz. The antenna has a directivity of 3.44 dBi at 2.4 GHz, and its 3 dB beamwidth is 89.8 degrees while at 3.5 GHz, the proposed antenna has a directivity of around 5.31 dBi and its 3 dB beamwidth is around 97.9 degrees. It can be observed that the antenna has broadside radiation pattern with bi-directional behaviour. The bowtie slot antenna is seen radiating at both front and back of the antenna. The antenna's directivity is also higher when at 3.5 GHz compared to when at 2.4 GHz. Additionally, the directivity of the antenna in Design A is seen to be higher than the reference antenna, indicating an increase in the radiation pattern's performance.

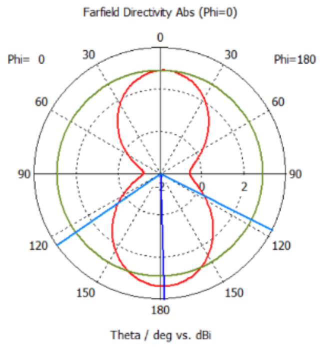

(a) xz plane at 2.4 GHz

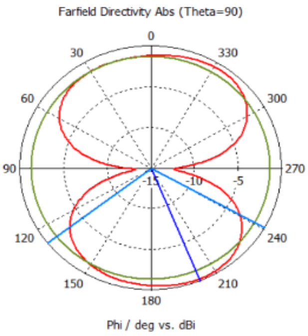

(b) xy plane at 2.4 GHz

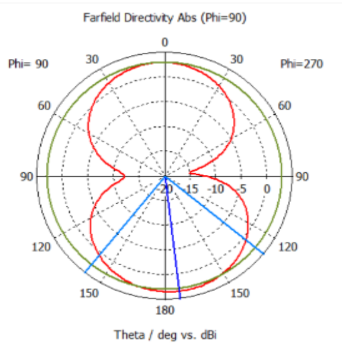

(c) yz plane at 2.4 GHz

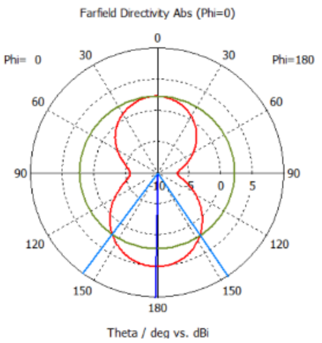

(d) xz plane at 3.5 GHz

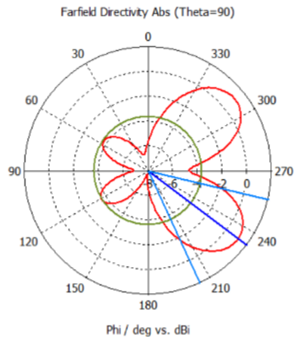

(e) xy plane at 3.5 GHz

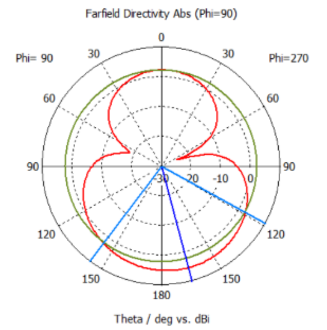

(f) yz plane at 3.5 GHz

Fig. 8 *Simulated 2D radiation pattern of Design A*

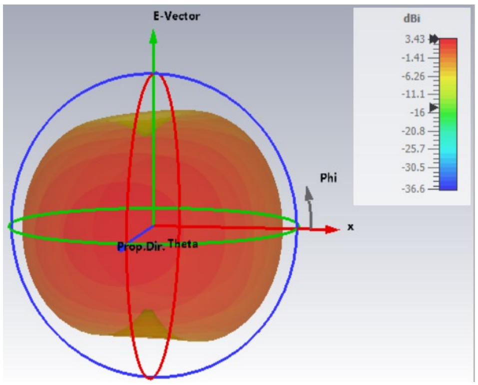

(a)

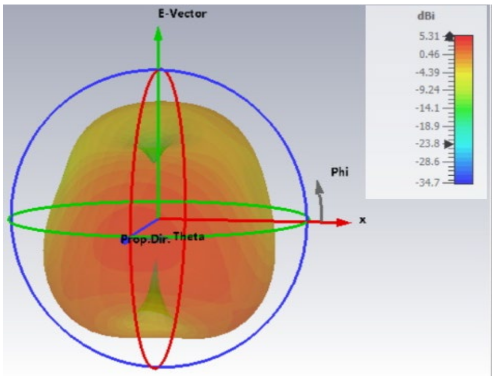

(b)

Fig. 9 *Simulated 3D radiation pattern of Design A at (a) 2.4 GHz (b) 3.5 GHz*

The simulated 2D and 3D radiation patterns for Design B are shown in Fig. 10 and 11. Design B displays a bi-directional radiation pattern performance, similar to Design A's radiation behaviour at 2.4 GHz and at 3.5 GHz. The proposed bowtie slot antenna has a directivity of approximately 3.37 dBi at 2.4 GHz and its 3 dB beamwidth is around 118.1 degrees. The antenna's directivity is around 5.05 dBi at 3.5 GHz, while the half power angular width of the antenna is about 70.2 degrees. Design B's antenna has a slightly higher directivity performance compared to Design A which shows that by introducing another slot to the ground plane, the antenna become slightly more directional and therefore, possesses higher directivity.

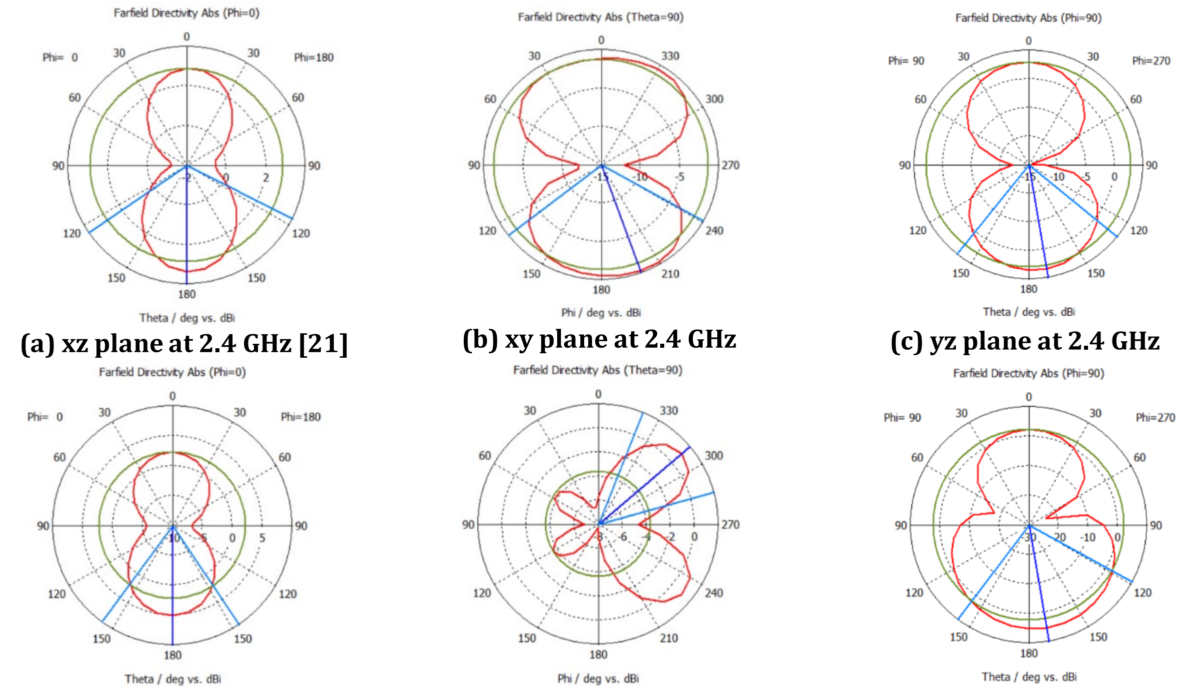

(a) xz plane at 2.4 GHz [21] **(b) xy plane at 2.4 GHz** **(c) yz plane at 2.4 GHz**

(d) xz plane at 3.5 GHz [21] **(d) xy plane at 3.5 GHz** **(d) yz plane at 3.5 GHz**

Fig. 10: *Simulated 2D radiation pattern of Design B*

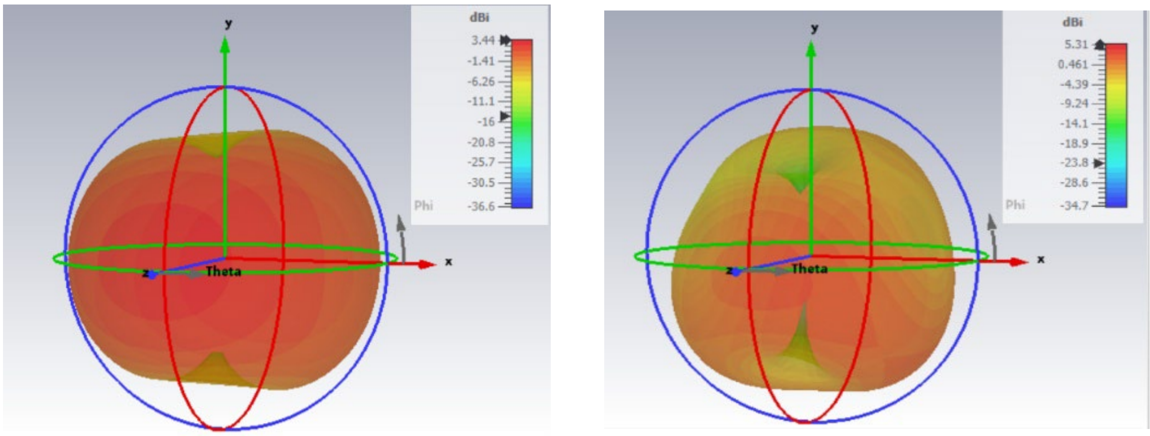

(a) **(b)**

Fig. 11 *Simulated 3D radiation pattern of Design B at (a) 2.4 GHz (b) 3.5 GHz*

The simulated radiation pattern performance of Design C can be found in Fig. 12 and 13 for 2D and 3D plots respectively. The antenna in Design C with circular slot has a directivity of around 3.43 dBi at 2.4 GHz and its 3 dB beamwidth is around 89.6 degrees. The antenna's directivity is around 5.28 dBi at 3.5 GHz, while the half power angular width of the antenna is about 98 degrees. Similar to Design A and Design B, the proposed antenna in Design C exhibits a bi-directional behaviour, radiating at front and back of the antenna. There is no significant improvement for Design C as compared to Design B. This indicates that there is no significant impact to the radiation pattern due to changing the pattern of the slot at the ground plane, as long as there is a defected structure at the ground plane at that particular point, regardless of the shape whether rectangular or circular, the radiation pattern is not impacted.

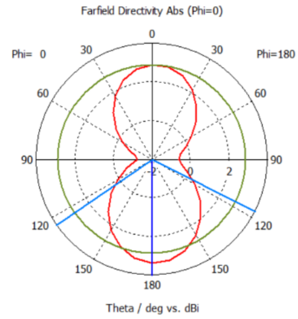

(a) xz plane at 2.4 GHz

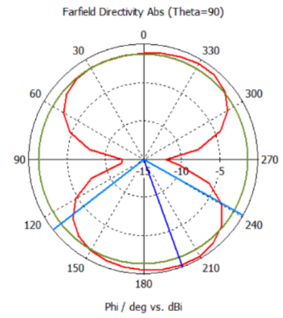

(b) xy plane at 2.4 GHz

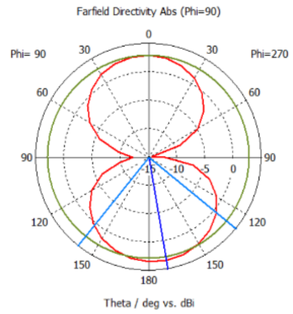

(c) yz plane at 2.4 GHz

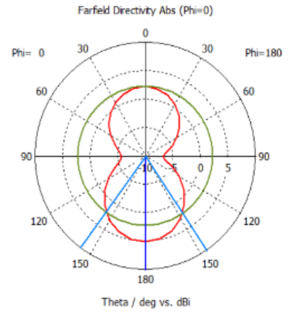

(d) xz plane at 3.5 GHz

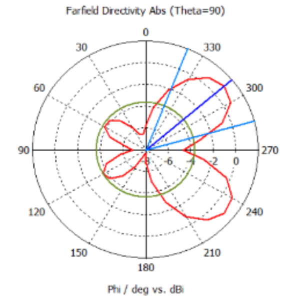

(e) xy plane at 3.5 GHz

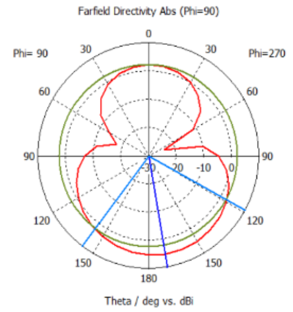

(f) yz plane at 3.5 GHz

Fig. 12 *Simulated 2D radiation pattern of Design C*

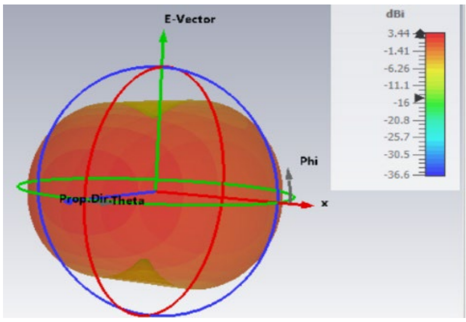

(a)

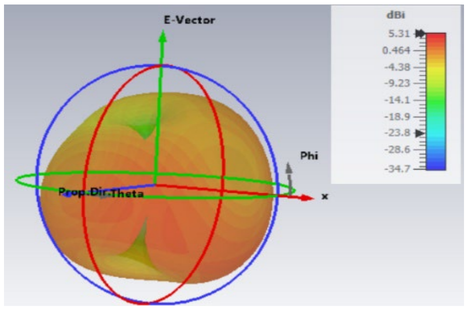

(b)

Fig. 13 *Simulated 3D radiation pattern of Design C at (a) 2.4 GHz; (b) 3.5 GHz*

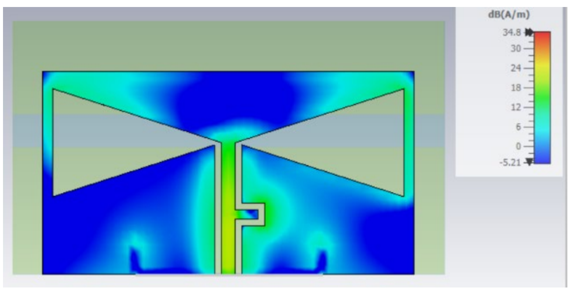

(a)

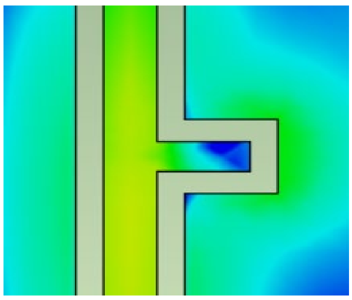

(b)

Fig. 14 *Simulated surface current flows on the top surface of the bowtie slot antenna at 2.4GHz [21] (a) top surface of the antenna; (b) closed up view of the ACPW*

The working mechanism of ACPW that was inserted into the bowtie slot antenna design is studied by observing the surface current flow of the antenna on the top surface [21]. Fig. 14 shows the surface current distribution of the proposed dual band bowtie slot antenna on the top surface where the design is maintained consistent for all design presented in the paper. It can be observed that on the top surface, the current flowing along the bowtie slot and the ACPW structure. This current flow caused a rise in the total capacitance [22]. The capacitance is influenced by the width of ACPW (length of W1), where an increase in W1 length results in higher capacitance [22]. This increase therefore results in reduction of the antenna's resonant frequency. This is also confirmed in Fig. 14 that shows the peak current flow occurs along the bowtie slot edges.

Fig. 15 investigates the distribution of the surface current at the bottom surface of the antennas in this work, especially studying the effect of inserting defected structures onto the ground at the bottom of the antenna. In Fig. 15(a) and (d), the current distribution is mainly impacted by the bowtie-shaped slot that was inserted onto the patch antenna on the top surface as there is no DGS added for the full ground design. The peak current flow occurs mostly near the feedline of the antenna with full ground. Fig. 15(b) and (e) display the surface current distribution for Design A at 2.4 GHz and 3.5 GHz respectively. It can be seen that the current at the ground plane were not able to flow freely on the ground surface. The current flow is cut off and discontinued due to the horizontal rectangular DGS, cutting off the current distribution into 2 separated sections. The rectangular slot in Design A successfully disrupts the flow of current on the ground plane. This gives rise to the total capacitance of the antenna design and minimizes the mutual coupling between the patch on the top and the ground plane on the bottom. This also explains the significantly improved bandwidth and reflection coefficient performance of the antenna in Design A as compared to the reference antenna with full ground as can also be observed in Fig. 5.

The simulated distribution of surface current of Design B is presented in Fig. 15 (c) at 2.4 GHz and (f) at 3.5 GHz. As expected, the current flow is disrupted to peak at the surrounding edge of the vertical rectangular slot upon introduction of another defected structure on the ground plane. The vertical DGS is placed directly beneath the microstrip feed line, altering its capacitance and inductance by accounting for the capacitance, resistance and inductance of the slots [15]. This phenomenon again improves and minimizes the antenna's reflected waves as can be noted previously in Fig. 5.

In Fig. 15 (g) and (h), the simulated distribution of surface current of Design C is displayed. These plots showed that as the current flowed in a circular motion surrounding the circular DGS, the current on the surface alters its movement path. This is also similar to the case in Design B where the current flow on the ground plane was disturbed and altered due to the presence of the two slots.

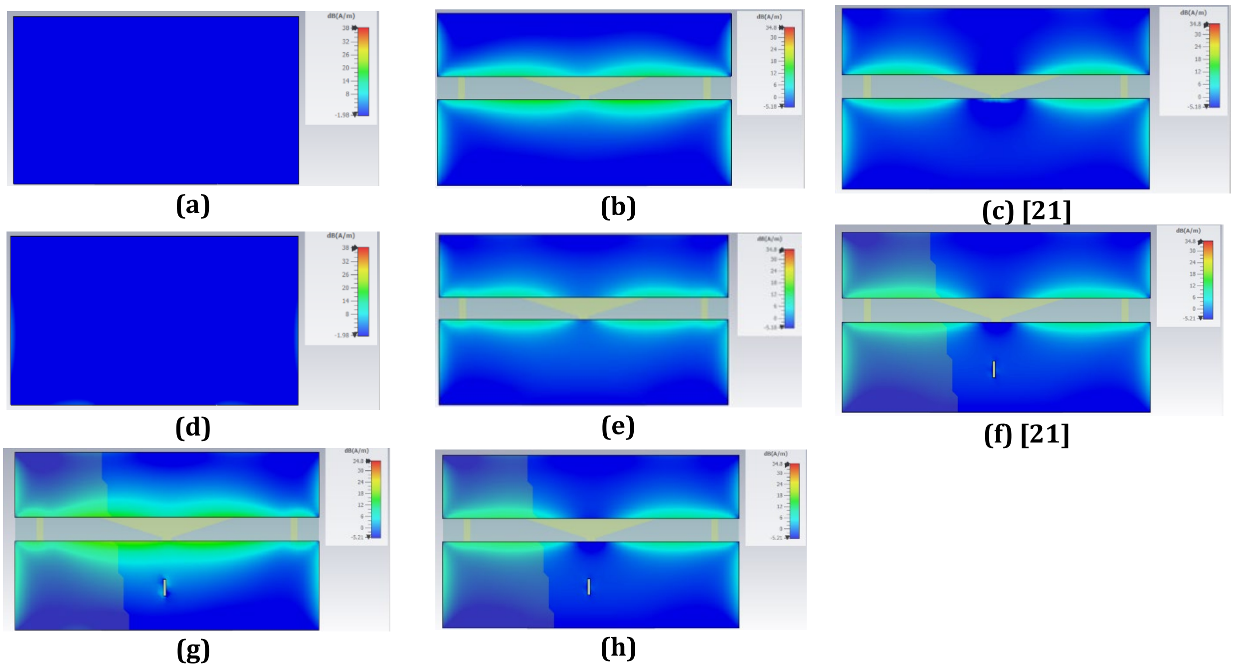

Fig. 15 *Simulated surface current distribution on the bottom surface of antenna for (a) full ground at 2.4 GHz; (b) Design A at 2.4 GHz; (c) Design B at 2.4 GHz [21]; (d) full ground at 3.5 GHz; (e) Design A at 3.5 GHz; (f) Design B at 3.5 GHz [21]; (g) Design C at 2.4 GHz; (h) Design C at 3.5 GHz*

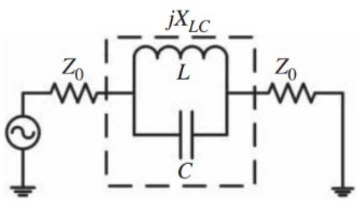

Fig. 16 *Equivalent LC model of a dumbbell DGS [21]*

This study demonstrates that the defected structure on the ground plane disturbs the flow of the surface current on the ground plane, influencing the reflection coefficient performance of the antenna. The primary goal of incorporating a defected structure on the ground plane is to interfere with the flow of the surface current. Additionally, DGS modifies the antenna's electric and magnetic fields, particularly on the ground plane, which increases the impedance matching and reduces the reflection waves between the antenna and the feed line. These findings can be represented using an equivalent schematic circuit consisting of a pair of equivalent capacitance and inductance model (LC model), as illustrated in Fig. 16 [21]. The placement of the DGS was found to be crucial, as positioning it under the feedline helped reduce the mutual coupling of the antenna design.

Previous related research work on simulated multi-band bowtie slot antenna is shown in Table 2. It can be seen that the bowtie antenna presented in Design C has the lowest reflection coefficient and higher directivity value compared to previous studies.

Table 2 *Comparison of previous bowtie slot antenna designs with multiband operation*

Reference	Resonant Frequency (GHz)	S_{11} (dB)	Bandwidth (GHz)	Directivity (dBi)
[23]	2.4	-24	11.43	N/A
	3.5	-18		N/A
[24]	2.4	-14	1.1	N/A
	2.86	-22		3.64
[18]	2.98	-28.5	0.97	3.7
	3.5	-10		
[21]	2.4	-68.7	0.605	3.37
	3.5	-67.9	0.845	5.05
This work (Design C)	2.4	-70.1	0.602	3.43
	3.5	-59.5	0.848	5.28

4. Conclusion

This paper investigates and compares the impact of the defected ground structure on the 2.4 GHz/3.5 GHz dual frequency bowtie slot antenna. This research intends to be applied for Wi-Fi and 5G applications, operating at two frequency bands, 2.4 GHz and 3.5 GHz. The research explored various combinations of the defected ground structure with different shapes. The findings revealed that the DGS integrated dual-band bowtie slot antennas studied in this research work exhibited outstanding reflection coefficient performance, reaching nearly -70 dB, compared to the reference design with a full ground plane. The study performed on the antenna parameters revealed that the dimensions of the DGS, particularly its length and width, had a noticeable effect on the operating frequency of the dual-band antenna design. For optimal dual-band performance, the horizontal DGS's length was fixed to become similar to the antenna's ground structure length. This adjustment is crucial as the DGS alters the magnetic and electric fields of the antenna, leading to a reduction in the antenna's reflected waves. Additionally, the placement of the DGS was found to be important, as positioning it under the feedline helped reduce the mutual coupling of the antenna design. The study presented in this paper is only simulation work. In the future, the simulated dual band bowtie slot antenna design will be fabricated, tested and measured to verify and validate the simulation results.

Acknowledgement

The authors would like to acknowledge the facilities and assistance provided by School of Electrical and Electronic Engineering, Universiti Sains Malaysia.

Conflict of Interest

Authors declare that there is no conflict of interest regarding the publication of the paper.

Author Contribution

*The authors confirm contribution to the paper as follows: **Design and simulation of the antenna:** Richard Ting Sing Wee; **Data collection:** Richard Ting Sing Wee; **Analysis and interpretation of results:** Richard Ting Sing Wee, Intan Sorfina Zainal Abidin, Azniza Abd Aziz; **Draft manuscript preparation:** Richard Ting Sing Wee, Intan Sorfina Zainal Abidin. All authors reviewed the results and approved the final version of the manuscript*

References

[1] Ali F, Salih M, Ilyas M. MIMO patch antenna with metamaterial 3.5ghz for 5G applications. 2022 Second International Conference on Advances in Electrical, Computing, Communication and Sustainable Technologies (ICAECT). 2022 April 21.

[2] Parchin, N. O., Basherlou, H. J., & Abd-Alhameed, R. A. Dielectric-insensitive phased array with improved characteristics for 5G mobile handsets. Progress In Electromagnetics Research M, 94, 209-219, 2020.

[3] Public policy position - huawei, https://www-file.huawei.com/media/CORPORATE/PDF/public-policy/Public_Policy_Position_5G_Spectrum_2020_v2.pdf?la=en (accessed September. 8, 2023).

[4] W. Xiang, K. Zheng, and X. (Sherman) Shen, 5G Mobile Communications. Springer Int. Publishing, 2018.

[5] Hongwei Wang, Guangli Yang. Design of 4×4 microstrip quasi-yagi beam-steering antenna array operation at 3.5GHz for future 5G vehicle applications. 2017 International Workshop on Antenna Technology: Small Antennas, Innovative Structures, and Applications (iWAT), 2017.

[6] Ashish J, Rao AP. Design and implementation of compact dual band U-slot microstrip antenna for 2.4GHz WLAN and 3.5GHz wimax applications. 2019 International Conference on Smart Systems and Inventive Technology (ICSSIT). 2019 November.

[7] Yassin AA, Saeed RA. Reconfigurable dual band antenna for 2.4 and 3.5 GHz using single PIN diode. 2013 International Conference on Computing, Electrical and Electronic Engineering (ICCEEE). 2013 August.

[8] S. M. Asha Banu, M. Ramkumar, and B. M. Shankar, “Hybrid optimization of graphene based dual band bow-tie microstrip patch antenna to detect breast cancer using Deep Learning Technique,” *Materials Science in Semiconductor Processing*, vol. 185, p. 108861, Jan. 2025. doi:10.1016/j.mssp.2024.108861

[9] T. Kumari, A. Senapati, and A. N. Ghazali, “Metasurface reflector-inspired directional bow-tie antenna for IOT and wireless applications,” Optik, vol. 327, p. 172309, May 2025. doi:10.1016/j.ijleo.2025.172309

[10] M.-J. Nie, X.-X. Yang, G.-N. Tan, and B. Han, “A compact 2.45-GHz broadband rectenna using grounded coplanar waveguide,” IEEE Antennas and Wireless Propagation Letters, vol. 14, pp. 986–989, Dec. 2015. doi:10.1109/lawp.2015.2388789

[11] V. Singh et al., “Design and performance measurement of microstrip slot antenna,” 2025 International Conference on Next Generation Communication & Information Processing (INCIP), pp. 217–221, Jan. 2025. doi:10.1109/incip64058.2025.11018947

[12] Balanis CA. Antenna Theory Analysis and Design. Newark: John Wiley & Sons, Incorporated; 2016.

[13] Mekki S, Zebiri C, Sayad D, Elfergani I, Bendjedi H, Rodriguez J, et al. A miniaturized slot antenna with defected ground structure for GSM applications. 2021 IEEE 26th International Workshop on Computer Aided Modeling and Design of Communication Links and Networks (CAMAD). 2021 October.

[14] Faouri YS, Salim A, Baqaleb S. Quad frequency rejection bands UWB bowtie microstrip antenna. 2020 IEEE International Symposium on Antennas and Propagation and North American Radio Science Meeting. 2020.

[15] Zeng Z, Cao W, Lv X. Triple-band triple-mode microstrip endfire antenna based on periodic bowtie dipoles, Sixth Asia-Pacific Conference on Antennas and Propagation (APCAP), 2017

[16] A. Singh and S. Joshi, “Design of Y-shaped tri-band rectangular slot dgs patch antenna at sub-6 ghz frequency range for 5G communication,” Journal of Engineering and Applied Science, vol. 71, no. 1, Jul. 2024. doi:10.1186/s44147-024-00476-w

[17] Guha, D., Kumar, C., & Biswas, S. (2023). Page 6,75, Defected Ground Structure (DGS) based antennas: Design physics, engineering, and applications. John Wiley & Sons, Incorporated.

[18] F. Arshad and H. Tenhunen, A Bowtie Slotted Quad-Band Notched UWB Antenna with Defected Ground Structure. ACES Journal, Nov 2019:34(11),1725-30

[19] Gopi D, Vadaboyina AR, Dabbakuti JR. DGS based monopole circular-shaped patch antenna for UWB applications. SN Applied Sciences. 2021 January 25;3(2).

[20] Dian Widi Astuti et al., "Bandwidth enhancement for half mode substrate integrated wave guide antenna using defected ground structures," International Journal of Electronics and Telecommunications, Sep. 2023. doi:10.24425/ijet.2023.144382

[21] Ting, Richard Sing Wee, Intan Sorfina Zainal Abidin, and Azniza Abd Aziz. Design of Dual Band Bowtie Slot Antenna with Rectangular-Shaped Defected Ground Structure. Journal of Physics: Conference Series. Vol. 2922. No. 1. IOP Publishing, 2024.

[22] Xu L, Li L, Zhang W. Study and design of broadband bow-tie slot antenna fed with asymmetric CPW. IEEE Transactions on Antennas and Propagation. 2015 February;63(2):760–5.

[23] Rashid S, Yizhi Wu, Yongsheng Ding. Monopole-like bowtie slot antenna for ultrawideband applications. 2016 IEEE International Conference on Computational Electromagnetics (ICCEM). 2016 February.

[24] Dayo Z, Cao Q, Wang Y, Soothar P, Khoso I, Shah G, et al. A compact high gain multiband bowtie slot antenna with miniaturized triangular shaped metallic ground plane. Applied Computational Electromagnetics Society. 2021 Aug 19;36(7):935–45.